# On rolling contact fatigue of gear steels with different inclusion content

**Donzella G.[1], Faccoli M.[1], Mazzù A.[1], Petrogalli C.[1], Desimone H.[2]**

[1]Università degli Studi di Brescia, Dipartimento di Ingegneria Meccanica e Industriale, via Branze, 38, 25123, Brescia, giorgio.donzella@ing.unibs.it
[2]Tenaris Dalmine, hdesimone@dalmine.it

**ABSTRACT.** *This work analyses the evolution of rolling contact fatigue damage in ring specimens made of quenched and tempered SAE 5135 steel for gears, obtained with three different steel-production processes.*
*The investigation was carried out through a test campaign on a bi-disk machine under pure rolling condition and water lubrication. Early formation of micro-pits, increasing in number with the test progression and joining forming larger pits was observed on the rolling surface, while the final failure was always caused by macro-spalling phenomena. The analysis of the specimens section allowed observing the complex pattern of surface and subsurface cracks and the role of inclusions in favouring crack nucleation and propagation. An analysis of inclusion content by means of extreme value statistics was also carried out referring to the three different steel-production processes and a relationship between RCF life and maximum expected inclusion size was highlighted.*

## INTRODUCTION

Rolling contact fatigue (RCF) of hardened steels, especially for gears, bearings and cams application, has been widely studied in the past [1]. Several damage phenomena have been observed in these components, mainly imputable to surface or sub-surface cracks initiation and propagation. Surface cracks are greatly affected by the working conditions and in particular favoured by the presence of sliding and lubricant pumping effect [2]. In hard materials, their initiation is mainly related to the stress concentration effect of asperities or near surface inclusions. Subsurface cracks originate in the bulk hertzian stress zone, growing preferentially by shear, almost parallel to the rolling surface [3]. Their initiation is also greatly favoured by the presence of inherent defects like inclusions, which act as stress raisers. This effect has been directly observed [4], artificially reproduced [5] and numerically simulated [6]. It was also recognised that subsurface RCF is a failure mechanism typical of hard materials, just because they are more sensitive to inherent defects, while in soft materials extensive plasticization nullifies their stress concentration effect. Surface and sub-surface RCF often appear at the same time, as independent phenomena. For example, in bearings under pure rolling

condition, an initial micropitting is commonly observed, but then it stops being the failure caused by subsurface initiated spalling [7]. Nevertheless, these two damage mechanisms can have sometimes a synergic effect and correspondent cracks join together.

As inclusions play a fundamental role in RCF of hardened steels [8], design criteria against RCF can be proposed which consider them as equivalent early formed cracks and define the RCF limit in terms of their propagation threshold, according to the short cracks theory [9]. The material production process becomes therefore crucial for these applications and its goodness in this sense can be judged by an analysis of the inclusion content. It is however quite complex to find a quantitative relationship between inclusion content and RCF resistance and in particular to predict which improvement in terms of RCF life can be achieved throughout a certain process refinement. This paper deals with this latter aspect, studying experimentally the RCF behaviour of typical steel for gears, obtained with three slightly different industrial processes. For this aim, some ring specimens were constructed and subjected to RCF tests. The damage evolution on the specimens has been studied and their life determined. A statistical analysis of the inclusion content has been also carried out for the three processes and a relationship between RCF life and maximum expected inclusion size has been searched for.


**RCF TESTS**

The tests were carried out on a high performances PC controlled *bi*-disk machine equipped with two independent mandrels, one of which translating on linear slides by means of a servo-hydraulic actuator. The specimens are ring shaped, machined from the same tubes used for the gears productions, made of hardened and tempered SAE 5135 steel. They present an inner diameter of 148 mm, an outer diameter of 175 mm and a thickness of 10 mm. Three series of specimens were constructed, hereafter named 'A', 'B' and 'C', obtained with different facilities and steel-practices and therefore containing three different grades of inclusion, as will be reported later. A counteracting disk with diameter of 65 mm, made of quenched and tempered 100Cr6 steel having hardness of 60 HRC, is mounted during the tests against the ring specimens, constituting a common reference. The RCF tests were carried out in pure rolling condition with water lubrication. Three hertz contact pressure levels $p_o$ was considered, namely 2000, 2200 and 2400 MPa. The rolling speed of the counteracting disc was set to 500 r.p.m., to which corresponds a ring-specimen rolling speed of 185 r.p.m.. Each test was continued up to the occurrence of severe RCF phenomena. At the test end, the specimens were cut along transversal sections (perpendicular to the ring axis) and observed by optical and electron microscope in order to analyze the damage under the surface. EDS analyses of the most significant inclusions were also carried out.

Each specimen presented macro damage phenomena, like spalling, after a cycles number $N_F$ reported in Table 1.

Table 1. RCF life $N_F$

|  | $p_o$=2000 MPa | $p_o$=2200 MPa | $p_o$=2400 MPa |
|---|---|---|---|
| Specimen A | 761481 | 451852 | 364815 |
| Specimen B | 885926 | 511111 | 381481 |
| Specimen C | 816667 | 501852 | 428148 |

All specimens also showed a similar damage evolution on the rolling surface during the test, which can be synthesised in the phases described in the following.

Phase a: early appearance of micro-pitting phenomena with dimension of the order of a few tens of microns. An example is reported in fig.1.

Phase b: joining of some micro-pits giving origin to larger pits, as shown in the same fig.1, reaching a maximum dimension of the order of 1-2 mm.

Phase c: increasing of the pits number, but not of their maximum dimension.

Phase d: sudden occurrence of macro-spalling, with consequent test interruption. The failure covers almost the whole axial length of the ring, extending for an analogue distance in the circumferential direction, as shown in fig.2.
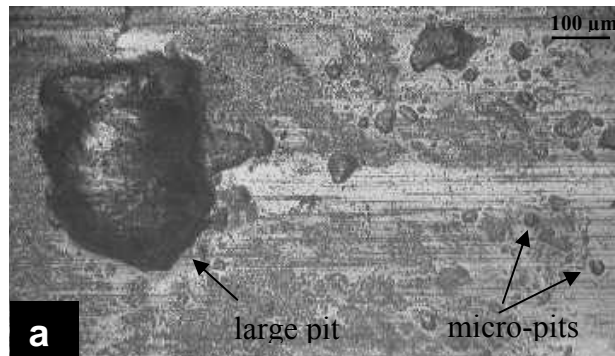


Figure 1. Example of pitting phenomena on the rolling surface
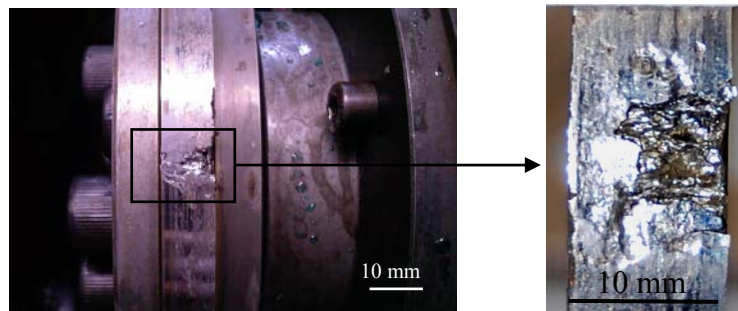


Figure 2. Example of spalling

It has been observed that spalling occurs without premonitory damage signs on the contact surface. This fact induces considering the spalling phenomenon as originated under the rolling track, due to the nucleation and propagation of subsurface cracks.

Furthermore, the presence of non propagating pits on failed specimens indicate that they are not the cause of the failure. The surface and subsurface damage mechanisms appear therefore as concomitant and independent. This result agrees with the experimental evidences observed by Cheng et al. [7] on a bearing steel.

Also in their sections, all the specimens presented a similar damage form. In fig. 3, an overview of a zone interested by the spalling is shown. A mean crack, almost parallel to the rolling surface and located at a depth of nearly 1 mm, can be observed. A complex crack layout accompanies the main crack; in particular, both several cracks starting from the surface and some isolated subsurface cracks can be noted.



Figure 3. Specimen section in the spalling zone

An example of subsurface isolated crack is shown in fig.4. Crack kinking is clearly visible, indicating, together with the crack orientation (parallel to the rolling surface), the presence of an important mode II propagation.
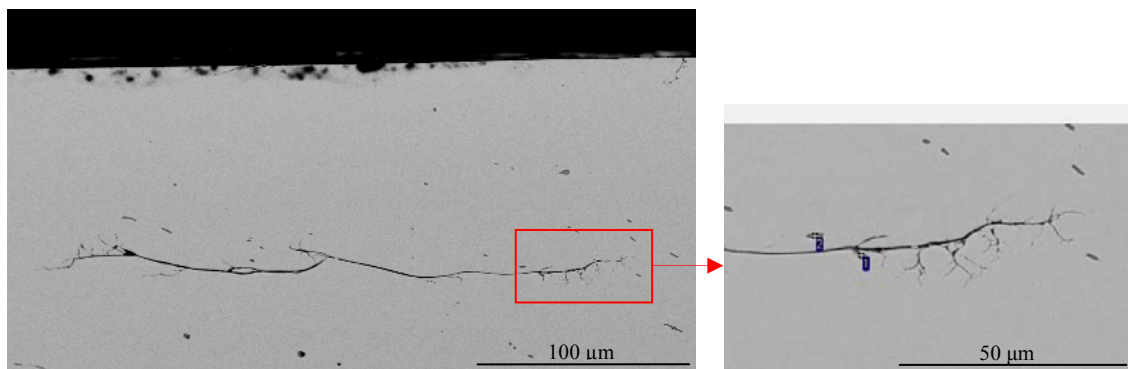


Figure 4. Isolated subsurface crack, growing in prevailing mode II

In fig. 5, a section of a large pit is shown, which presents a depth of about 80 μm. On the right, two smaller-pits are also visible, with comparable depth. A near-surface crack joining the bottom parts of the smaller pits is growing towards the large pit, showing an incipient de-attachment of material and consequent size increasing of the pit itself: this

786

observation confirms that large pits derive from progressive joining of micro-pits, interesting only the surface layer and not causing severe damage.
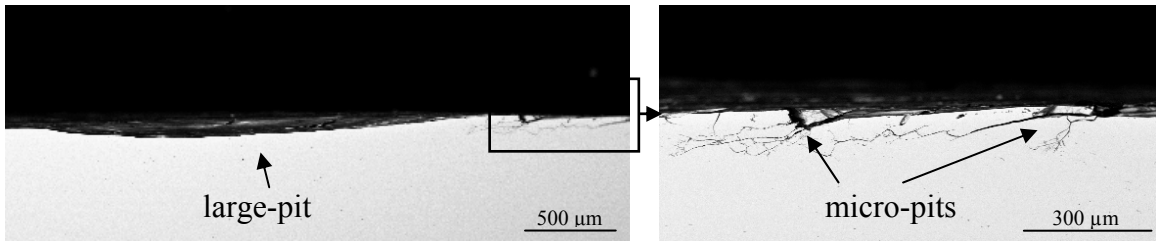


Figure 5. Mechanism of micro-pits joining, giving origin to large pits

The influence of inclusions on crack formation and layout is shown in the following figures. Figure 6 shows a typical surface crack growing with an angle of about 30° from the surface, which deviates its path in correspondence of a manganese sulfide.
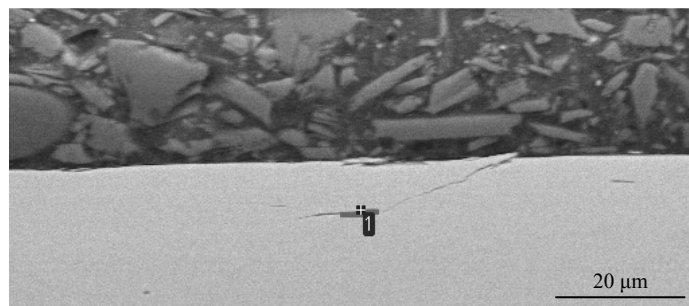


Figure 6. Surface crack deviating in correspondence of a manganese sulfide

Similarly, several inclusions (mainly manganese sulfides), were found on the path of deep sub-surface cracks, as can be seen in fig.7a, which shows some micro-cracks emanating from two adjacent sulfides and joining together.
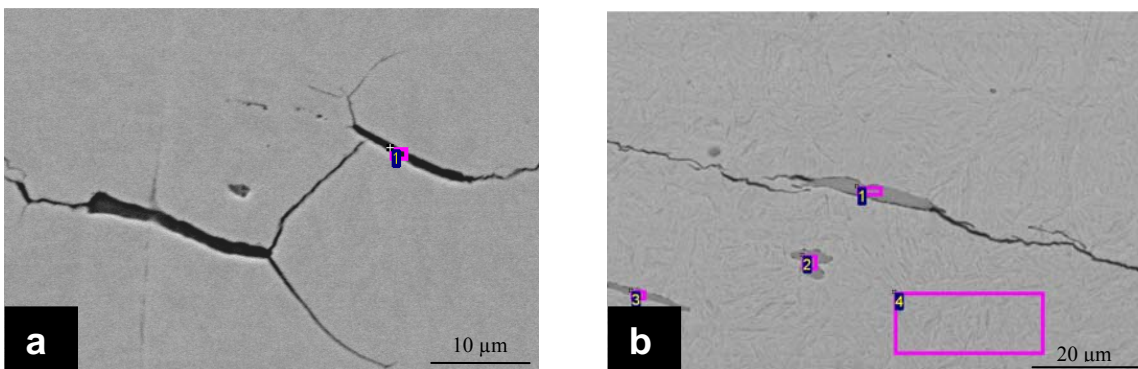


Figure 7. Subsurface isolated micro-cracks emanating from manganese sulfides

The important role of inclusions in favouring crack initiation and influencing their growth is confirmed and highlighted in some pictures taken from an additional type B specimen, tested at 2000 MPa only for a few thousand of cycles, i.e. stopped much before the spalling appearance and then sectioned in order to analyse the incipient RCF damage. Several isolated subsurface cracks were observed on this specimen, in one of which an important manganese sulfide was found (fig.7b). Cracks orientation (about 20°) coincides with that of the sulfide, but it is also compatible with a mixed mode I and mode II crack growth and agrees with some experimental evidences of subsurface micro-cracks propagation from inclusions [4].

## STATISTICAL ANALYSIS OF DEFECTS

In order to compare the effectiveness of the three steel-making processes under examination in terms of material cleanliness, a statistical analysis of the inclusion content was carried out through the large extreme value distribution technique [10], following [11] and [12]. The analysis was carried out on the transversal section of the specimens (normal to the ring axis), because this coincides with the main plane of crack propagation (mode I and mode II) for the specimen under examination.

Two types of inclusions were found for each steel-making process: manganese sulfides and mixed oxides (with manganese sulfides). Sulfides were always present in lengthened form; mixed oxides appeared in two different morphologies, according to the way in which the sulfide was arranged around them: globular and lengthened.

The results of the microscopic observations were analyzed separately for the two inclusion typologies above described, using the Gumble largest extreme value distribution and the method of moments. Figure 8 report the population of defects for the three steel-making processes examined, with the corresponding interpolating distributions and the 95% confidence bands.
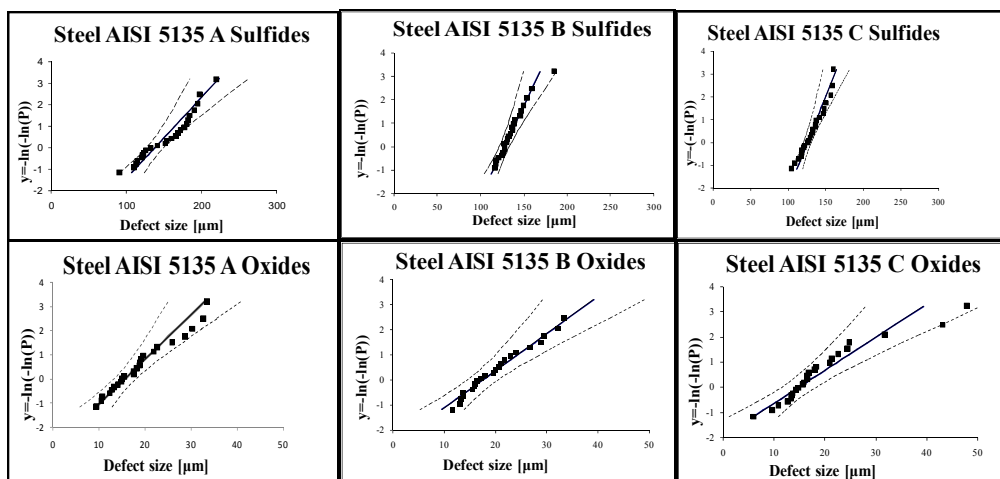


Figure 8. Inclusion distributions for the three steel-making processes

Table 2. Maximum expected inclusion size on the hertzian stress field area

| Steel-process | A | B | C |
|---|---|---|---|
| $L_{max}$ [µm] (sulfides) | 172,69 | 144,14 | 140,95 |
| $L_{max}$ [µm] (oxides) | 24,05 | 26,43 | 24,96 |

In Table 2, the maximum inclusion size expected on the hertzian stress field area of 550 mm$^2$ (calculated as that of a circular crown with a depth of 1 mm, comparable to the contact area half-width of the specimens) are reported, determined on the bases of the above defects distributions. A relationship between RCF life and maximum expected sulfides dimension is shown in fig.9. Although referring to the limited number of tests carried out, the figure indicates, as expectable, the existence of an inverse dependence between these two parameters, highlighted by the regression lines drawn in the graph. It can be also noted that the inclusion influence increases (i.e. the regression line presents a greater slope) at increasing pressure levels. The above considerations do not apply to the oxides, which present significantly smaller dimensions.
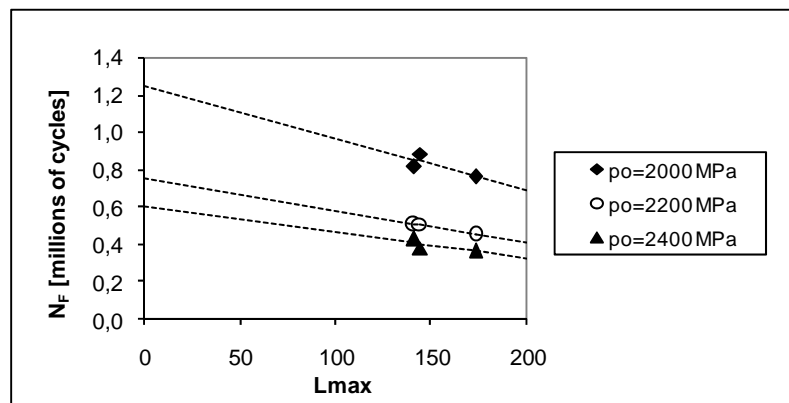


Figure 9. Relationship between RCF life and maximum expected sulfide size

**CONCLUSIONS**

Two main damage mechanisms were recognised on the specimens:
- a surface RCF, consisting in the propagation and early branching of inclined surface cracks, under the action of the contact stress field and the pumping effect of the water inside the crack faces. This mechanism is thought responsible for micro-pits formation, and their subsequent joining to create larger pits;

- a subsurface RCF, consisting in the prevailing mode II propagation of cracks parallel to the surface or slightly inclined with respect to it, under the action of the bulk herztian stress field. This mechanism leads to the spalling phenomenon.

The two mechanisms appear as independent, but in some way synergic, as a complex pattern of secondary cracks develop between the main crack and the surface, weakening the correspondent layer and favouring the de-attachment of important pieces of material.

Both mechanisms also appear influenced by the presence of inclusions, which can favour surface or subsurface crack formation and growth, define their initial orientation or change their path during propagation. This effect has been highlighted by the SEM analyses of the specimens sections, which show in some cases isolated micro-cracks propagating from inherent defects. As a confirmation of this interpretation, the extreme values statistical analysis of the inclusion content in the three examined steel-making processes gave results related to the corresponding RCF life.


## REFERENCES

1. Hyde, R.S. (1996), "*Contact fatigue of hardened steel*". In: *ASM Handbook* **19**.
2. Johnson, K.L., (1989) *Proc. Instn. Mech. Engrs.* **203**, 151-163.
3. Salehizadeh, H., Saka, N. (1992) *Journal of Tribology* **114**, 690-697.
4. Nélias, D., Dumont, M.L., Champiot, F., Vincent, A., Girodin,D., Fougères,R., Flamand,L., (1999), *Trans of the ASME* **121**, 240-251.
5. Donzella,G., Mazzù, A., Solazzi, L. (2001) "*Subcase Crack Propagation Threshold and Microhardness Profile Influence in Rolling Contact Fatigue of Carburised Components*" *Proc. 10th Intern. Conf. on Frac.*, 2-6 dec., Honolulu.
6. Melander, A. (1997) *Int. J. of Fatigue* **19**, N1, 13-24.
7. Cheng, W.W., Cheng, H.S. (1997). *Journal of Tribology* **119**, 233-240.
8. Auclair, G. et al. (1997). "*Cleanliness Assessment: a Critical Review and a Real need to Predict Rolling Contact Fatigue Behaviour*". *Proc. 5th Int. Symp. Bear. Steels*.
9. Bormetti, E., Donzella, G., Mazzù, A. (2002). *Tribology Transactions* **45**, 3, 274-283.
10. Beretta, S., Murakami, Y., (1998) *Fat. & Frac. Eng. Mat. & Struc*. **21**: 1049-1065.
11. ASTM E 2283 – 03.
12. ESIS P11 – 02.